

## Numerical simulation of the thermal behavior of natural fiber composite gears: case of HDPE 40

K.F. Wotodzo<sup>1</sup>, K.A. Kassegne<sup>2\*</sup>, D. Koffi<sup>3</sup> and S. Tiem<sup>4</sup>

<sup>1</sup>Département de Génie Mécanique, Ecole Nationale Supérieure d'Ingénieurs, Université de Lomé, B.P. 1515 Lomé, Togo

<sup>2</sup>Maître de Conférences, Département de Génie Mécanique, Ecole Nationale Supérieure d'Ingénieurs, Université de Lomé, B.P. 1515 Lomé, Togo

<sup>3</sup>Professeur Titulaire, Directeur du Pôle R&D Francophone sur les Engrenages en Plastique – Ecole d'ingénierie, Université du Québec à Trois-Rivières, CP 500, Trois-Rivières, Québec, G9A 5H7, Canada

<sup>4</sup>Professeur Titulaire, Département de Génie Mécanique, Ecole Nationale Supérieure d'Ingénieurs, Université de Lomé, B.P. 1515 Lomé, Togo  
kkassegn@yahoo.fr

Available online at: [www.isca.in](http://www.isca.in), [www.isca.me](http://www.isca.me)

Received 22<sup>nd</sup> July 2019, revised 12<sup>th</sup> September 2019, accepted 25<sup>th</sup> September 2019

### Abstract

*This study is the continuation of the work to adapt the wood fiber composite materials to the gears, to manufacture a new generation of gears and to predict the thermomechanical behavior of these gears. In this part we are interested in the thermal study. Simulation studies of thermal behavior led to the knowledge of the evolution of the equilibrium temperature and the instantaneous temperature on the tooth profile as a function of  $S/p_n$ , the normalized position of the contact point, by varying the wear rate. The distribution of the local instantaneous temperature  $T_{son}$  the Hertz contact width as a function of the position of the contact point along this width has also been studied. The study of the thermal behavior revealed that the instantaneous temperature is always higher than the equilibrium temperature on the profile of the tooth, except at the primitive point where the two temperatures are confused. Also, there is no significant difference between the instantaneous pinion and wheel temperatures and in addition the applied wear rates have no significant influence on the temperatures.*

**Keywords:** Composite, gears, natural fibers, modeling, temperature, MatLab.

### Introduction

The materials used to design the mechanisms are increasingly at the heart of research. It is essential, even vital, to identify all the contours of these materials. The field of study of the materials is very vast and deals as well with the metals and alloys, the ceramics as on the new materials like the polymers and composites. It is in fact to apprehend and better characterize the performance of these materials from their microstructure. Faced with the environmental and economic challenges of recent years, major research centers have embarked on the development and study of new materials such as polymers, composites, nano-composites of natural fibers, etc<sup>1-4</sup>. All these studies did not focus on the use of new materials for the manufacture of gears.

Our study, in fact, not only concerns a new material, but also its use in the manufacture of gears. Indeed, the gears are the most used machine elements in the power transmission systems and this, because of the multiple benefits they provide. The choice of polymers and their composites for the gears results in a noticeable reduction in production costs and makes it possible to envisage operating conditions without lubrication with attenuation of shocks and vibrations during the meshing of the teeth.

However, thermoplastic composites (such as HDPE 40), by the nature of the thermoplastic matrix, are very sensitive to

temperature. Thus these materials can see their mechanical characteristics deteriorate with the rise in temperature which is a mark of weakness for these materials because for these gears apart from the traditional forms of breakage encountered in the gears, is added thermal breakage.

Moreover, the operating conditions of these gears can be at the origin of certain damages such as the wear of the active surfaces. Statistics show that, in geared power transmission systems, the tooth concentrates more than 60% of the defects recorded. It is with this in mind that we propose to study the influence of wear and operating conditions on the distribution of equilibrium and surface temperature of the tooth in steady state.

### Materials and Methods

**Materials:** The composite that is the subject of this study is HDPE40 (high density polyethylene with 40% birch fiber), which production has been extensively detailed by Mijiyawa<sup>12</sup>. It is a composite whose matrix is plant-based polyethylene reinforced with 40% birch wood fiber with 3% MAPE (polyethylene maleate) as coupling agent.

**Modeling and computer simulation of equilibrium temperature  $T_b$  of gears made of thermoplastic reinforced with wood fiber:** Many numerical methods are proposed to predict the operating temperature of plastic and composite gears<sup>5-9</sup>. To do this, it is important to control the various

parameters of convection-diffusion in steady state, the method of the system of mesh finite-difference, as well as the definition of the equations on each node of the mesh.

**Two-dimensional steady-state convection-diffusion equation:** Two-dimensional steady-state temperature distribution in a variable-section body is obtained by applying the principle of energy conservation at every point of the body; this principle is expressed by the elliptic Poisson differential equation<sup>10</sup>:

$$\frac{\partial^2 T}{\partial x^2} + \frac{\partial^2 T}{\partial y^2} + \frac{qp(x, y)}{k} = 0 \quad (1)$$

T: Temperature, k: Thermal conductivity, qp (x, y): Rate of heat production in the body.

This equation will be solved numerically by the finite difference method.

Calculation of the heat flow rate requires knowledge of the conduction and convection heat flow rate. The rate of heat flow in conduction is calculated as follows:

$$q_c = -kA \frac{dT}{dx} \quad (2)$$

In convection, the following equation allows the determination of the heat flow rate:

$$q_{conv} = hA(-T_p + T_A) \quad (3)$$

With: A: the normal surface of heat exchange, h: the heat transfer coefficient,  $T_p$ : the temperature at the node at the surface,  $T_A$ : the ambient temperature near the body.

**Axis system and mesh:** A finite difference program is developed by Koffi for the numerical study of steady-state temperature distribution<sup>7</sup>. Figure-1 shows the geometry of the mesh used for the development of the program. I varies from 1

to  $N1 + 2$  while J varies from 1 to  $N2 + 2$ ,  $N1$  and  $N2$  denoting the number of internal nodes along the x axis and the y axis, respectively<sup>7</sup>.

**Thermal modeling - working hypothesis and application of heat transfer equations to gears:** For gears initially at ambient temperature, the gear system is gradually warmed until it reaches an equilibrium distribution after several cycles of operation. For each cycle, the loaded profile of the tooth undergoes an identical heat flow, the warming period at each cycle is extremely small compared to the cycle time. Then, at a given point on the profile, the tooth receives a heat pulse for each cycle. This causes a temperature fluctuation shown in Figure-2. It is this temperature pulse that diffuses through the tooth so that it reaches the equilibrium temperature.

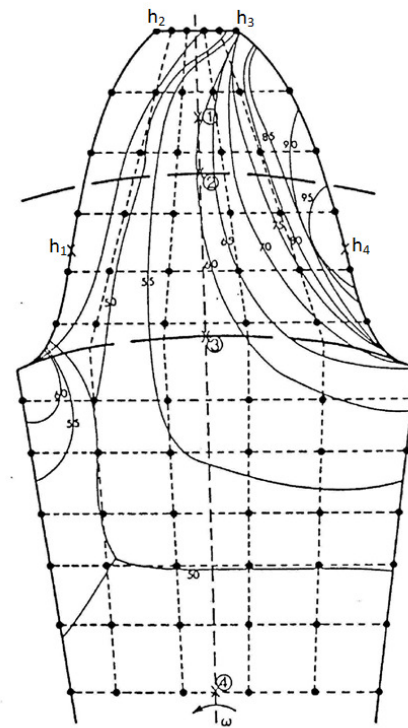
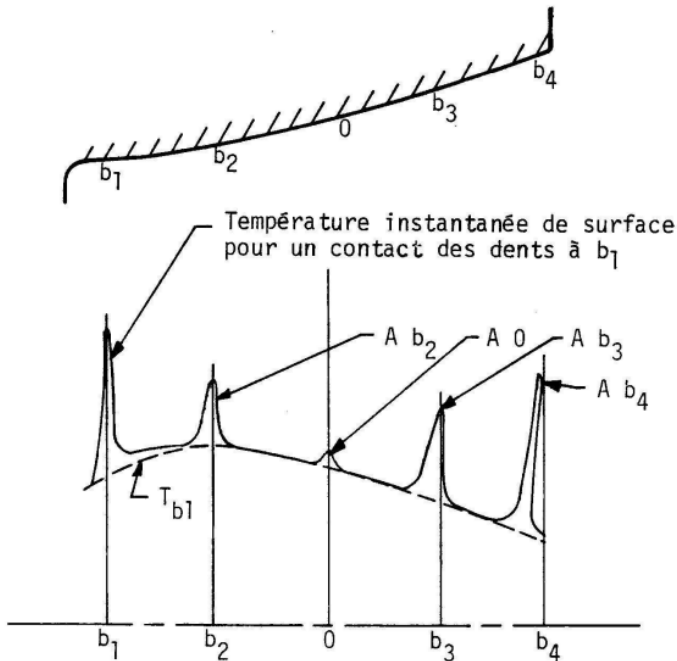


Figure-1: Mesh of geometry<sup>7</sup>.

**Table-1:** Values of heat transfer coefficients h (w / m<sup>2</sup> / s); Z = 30, α = 20°, v = 4m / s<sup>11</sup>

	Module, mm (pas P po <sup>-1</sup> )							
	5 (5.08)	*	8 (3.18)	*	10 (2.54)	*	12 (2.12)	*
h1	595	548	645	623	510	525	395	413
h2	500		600		540		430	
h3	395	475	500	585	435	455	340	380
h4	555		670		475		420	



**Figure-2:** Fluctuation of temperature on the tooth's loaded surface<sup>7</sup>.

Because of the repetitive nature of the production and heat-removal mechanisms for each tooth during the rotation of a gear, only one tooth is under study and the results are applicable to all other teeth of the same gear. The boundary conditions used are those of Wang and Cheng modified to limit the study to a tooth height under the foot circle of the gear<sup>7</sup>. This is justified by the fact that the temperature values of the foot circle towards the center of the gear are very close to the ambient temperature<sup>12</sup>.

**Finite difference method for determination of equilibrium temperature distribution: Numerical method:** The solution of the Poisson equation (1) is obtained using Liebmann's finite difference iterative method which derives from the method of successive Gauss Seidel displacements<sup>12</sup>. The Liebmann method ensures a rapid convergence of the solution by considering for the iteration of rank n during the calculation of the temperature T (I, J), the calculated values of the temperatures at the nodes whose numbers along the axes x and y are lower than I and J rather than considering the values of these same temperatures calculated at the iteration of rank n-1. Kirchhoff's law, which ensures the equilibrium of each node by canceling the effect of all the heat flux while considering that of any source of internal heat in steady state, is used to find the equations of the characteristic nodes; this law makes it possible to cancel the residues in each node and simplifies the numerical solution.

**Characteristic node equations:** We assume constant thermal conductivity of material k in all directions and that the distribution of the heat transfer coefficient is that established by

Akozan, which is illustrated in Figure-3. The characteristic equations at the nodes are amply detailed in the thesis of Koffi and Mijiyawa<sup>7,12</sup>.

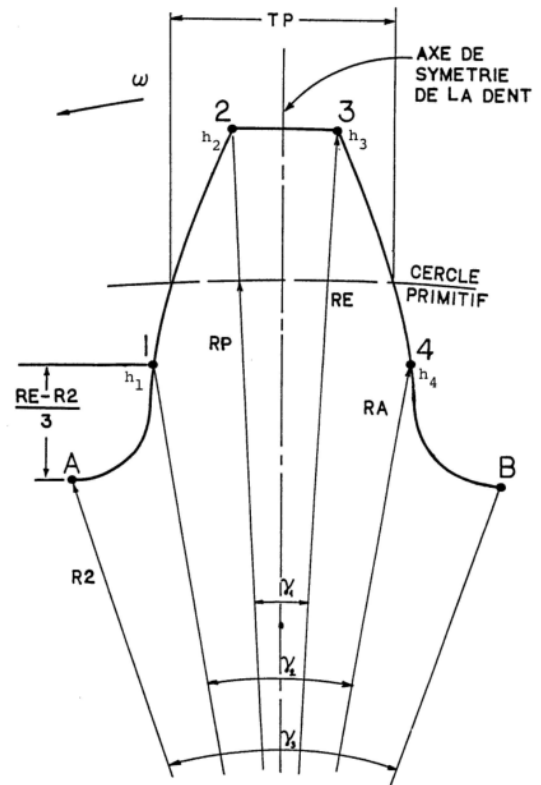


**Figure-3:** The points and angles considered by AKOZAN for calculating the heat transfer coefficient<sup>11</sup>.

Instantaneous temperature  $T_s$  at the surface of the tooth: This section presents the method for determining the local instantaneous temperature at the tooth surface during gears operation. This method involves applying the surface instantaneous temperature distribution equations of two semi-infinite solids to the gears.

Distribution of the surface instantaneous temperature of two infinite solids in contact: For two solids in contact with a moving non-uniform heat source at the contact surfaces, the instantaneous temperature rise of the body 1 and 2 at the  $x'$  position along the x-axis of the surface (Figure-4) express<sup>13</sup>:

$$\left\{ \begin{array}{l} \Delta T_1(x', t) = \frac{2\pi}{\pi \rho_1 c_1 \sqrt{\alpha_1}} \int_0^{\sqrt{t}} d\lambda \int_{\xi_{B1}}^{\xi_{H1}} \phi_1 q e^{-\xi^2} d\xi_1 \\ \Delta T_2(x', t) = \frac{2\pi}{\pi \rho_2 c_2 \sqrt{\alpha_2}} \int_0^{\sqrt{t}} d\lambda \int_{\xi_{B2}}^{\xi_{H2}} (1 - \phi_1) q e^{-\xi^2} d\xi_2 \end{array} \right. \quad (9)$$

With,

$$\left\{ \begin{array}{l} \lambda = \sqrt{t - \bar{t}} \\ \xi = \frac{x - \bar{x}}{\lambda \sqrt{4\alpha}} \\ x' = x - \bar{x} \\ \alpha = \frac{k}{\rho c} \end{array} \right.$$

Or:

$\alpha$  = thermal diffusion coefficient,  $k$  = thermal conductivity,  $\rho$  = density,  $c$  = specific heat,  $x_t$  = position of the center of the heat source at time  $t$ ,  $q$  = heat flux per unit area per unit of time,  $\phi_1$  = local heat distribution coefficient of the body 1,  $t$  = time after the start of contact.

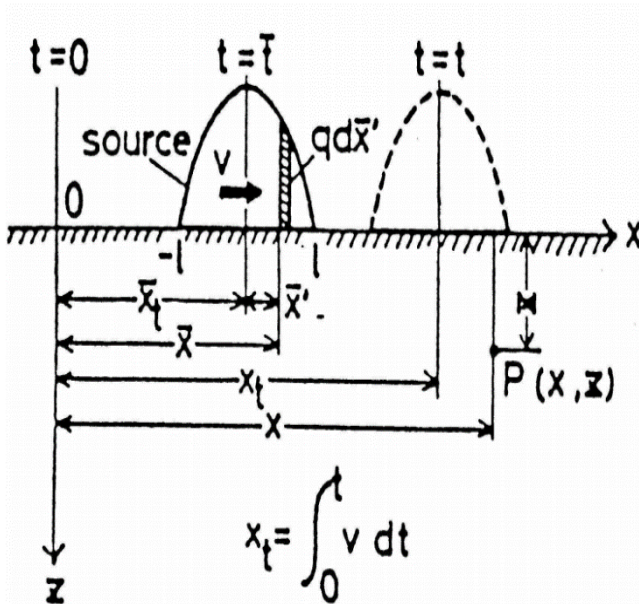


Figure-4: Heat source moving on the contact surface of two semi-infinite solids<sup>7</sup>.

The use of equations (9) assumes that the surface is subjected to the heat source at the position  $x = x_t$  on the surface at time  $t$ . When it is considered that the two surfaces are subjected to a Hertz contact of width  $2b$ , the heat flux for a given contact is then distributed between the positions  $x = -b$  at  $x = +b$  and the limits of the second integration in equations (9) are deduced as follows.

For the start of contact:

$$\zeta_A = \frac{x - x_t - b}{\lambda \sqrt{4\alpha}}$$

$$\zeta_B = \frac{x - x_t + b}{\lambda \sqrt{4\alpha}}$$

At each point of contact, the surface temperatures of the two bodies are equal and written:

$$T_{b1} + \Delta T_1 = T_{b2} + \Delta T_2 \quad (10)$$

The equation above is used to determine local heat distribution factors  $\phi_1$  and  $\phi_2$ . The average temperature rise over the contact width as well as the average heat distribution factor are expressed<sup>7</sup>:

$$\Delta T_m = \frac{1}{2b} \int_{-b}^{+b} \Delta T_1 dx' \quad (11)$$

$$\phi_m = \frac{\int_{-b}^{+b} \phi q dx'}{\int_{-b}^{+b} q dx'} \quad (12)$$

**Application to plastic gears:** The equations (9) applied to the geometry and motion of the gears give the instantaneous elevation of temperature on the profile of each of the teeth. The application of these equations requires the modification of certain parameters; in this particular case, the ones to be changed are: i.  $T = 0$ , the heat source at the initial time for each contact width  $2b$  of Hertz, ii.  $x_t = 0$ , the point of application of the source at the initial moment (point of contact) becomes the origin of  $x$  position on the profile of the tooth, iii.  $x_t$  = position of the contact point on the tooth profile at time  $t$ .

The solution is obtained using a numerical integration<sup>7,12</sup>.

**Description of the temperature calculation program and calculation algorithm:** The program was written in Matlab, translated and updated from FORTRAN. The original program was written in 1986 by KoffiDémagna (UQTR) and is also the continuation of the program pre-written by Fayçal Mijiyawa who had already begun the translation of the program<sup>7,12</sup>.

The program is in the form of script inside which there are 3 sub-scripts. The first sub-script calculates the heat of friction and hysteresis, the second script defines the geometry and the temperature configuration of the distribution model of the equilibrium temperature and calculates this distribution. Finally, the third sub-script calculates the distribution of the instantaneous temperature along the profile as well as the instantaneous factors of heat distributions for teeth 1 and 2.

**The structure of the flowchart for each of the scripts is as follows:** i. Sub-Script 1: calculates the different heats (Figure-5), ii. Sub-Script 2: calculates the steady-state temperature distribution (Figure-6), iii. Sub-Script 3: calculates the instantaneous temperature on the profile (Figure-7).

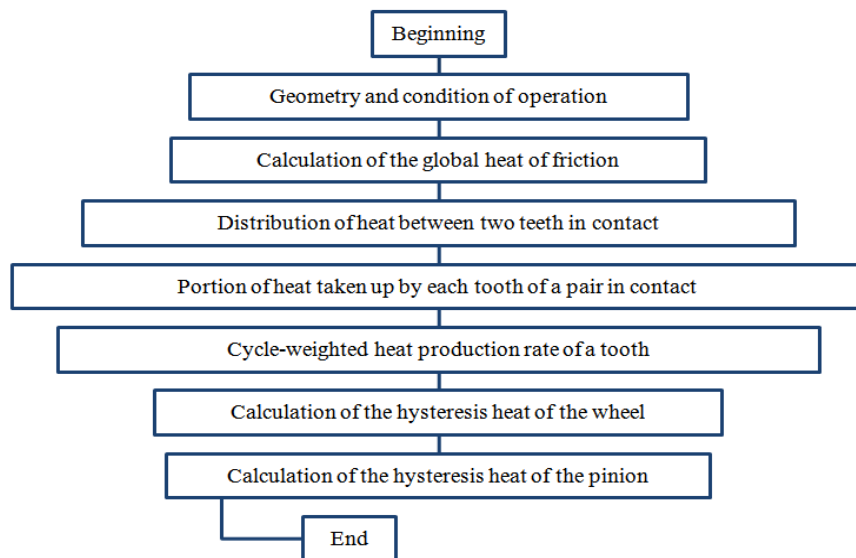


Figure-5: Organigramme Sub-Script 1: Heats calculation.

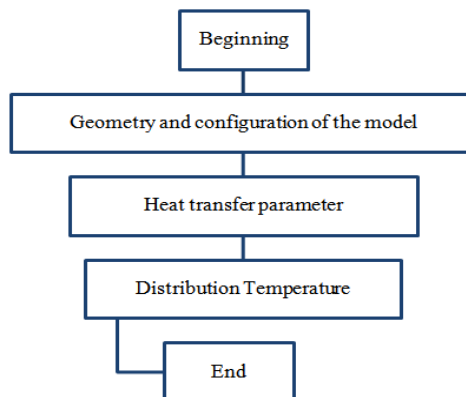


Figure-6: Calculation of the steady-state temperature distribution.

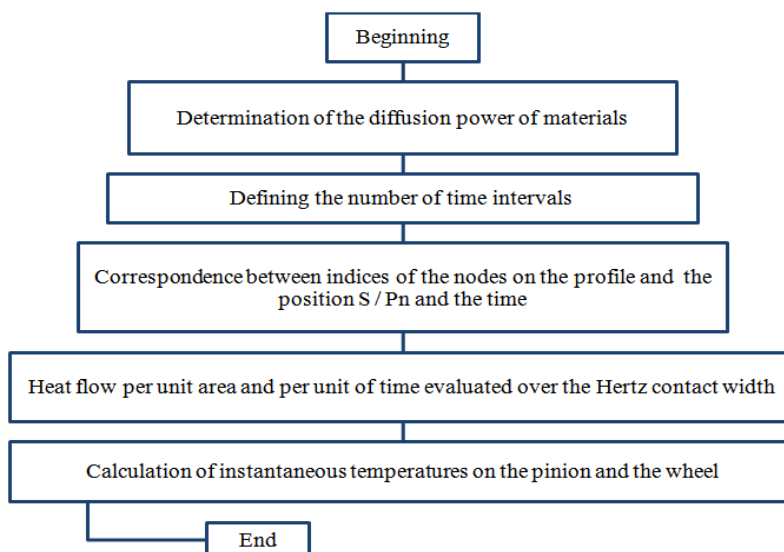


Figure-7: Sub-Script 3: calculation of instantaneous temperature on the profile.



**Results and discussion**

In this part, we present the results from the study conducted on temperature simulation and the resulting interpretations. The equilibrium and instantaneous temperatures are presented according to the wear rates of 0%, 4% and 8%.

All the geometry conditions of the gears, operating parameters and physical properties of the materials used in the tests carried out were introduced into the computer program for the simulation. Other conditions have been added (variation in wear rates) to broaden the range of parameter variation and to predict behavioral trends through equilibrium temperature and instantaneous temperature results. The results are as follows:

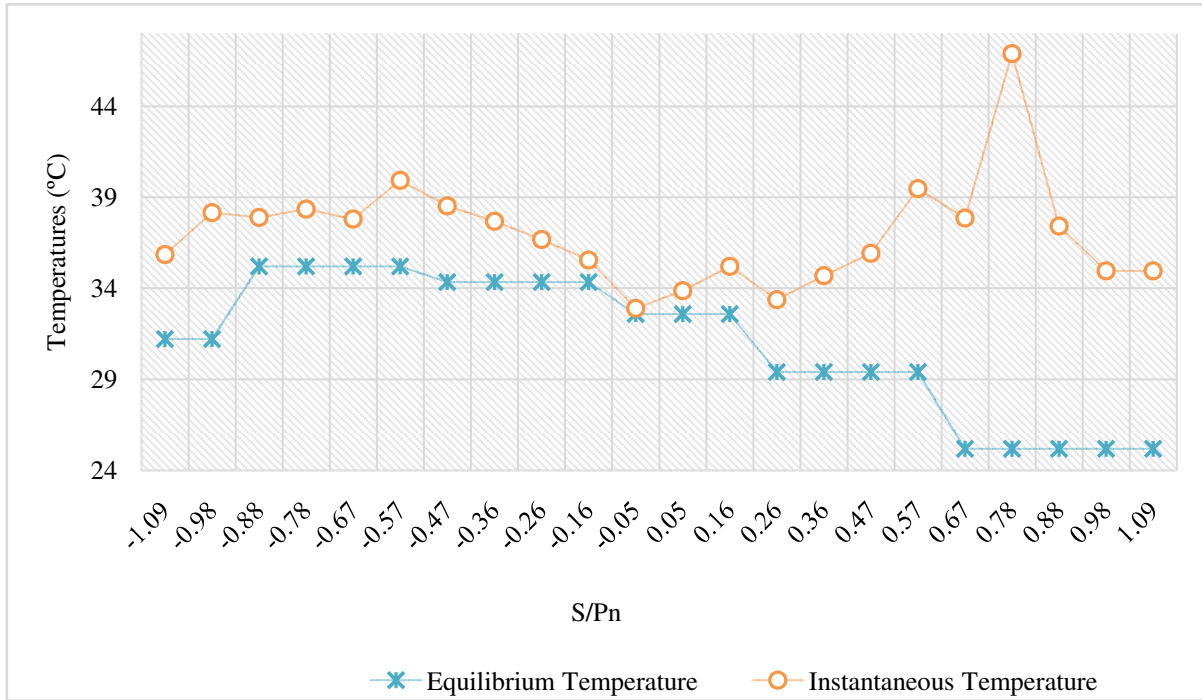


**Figure-8:** Instantaneous and equilibrium temperature variation on the pinion (0% wear).

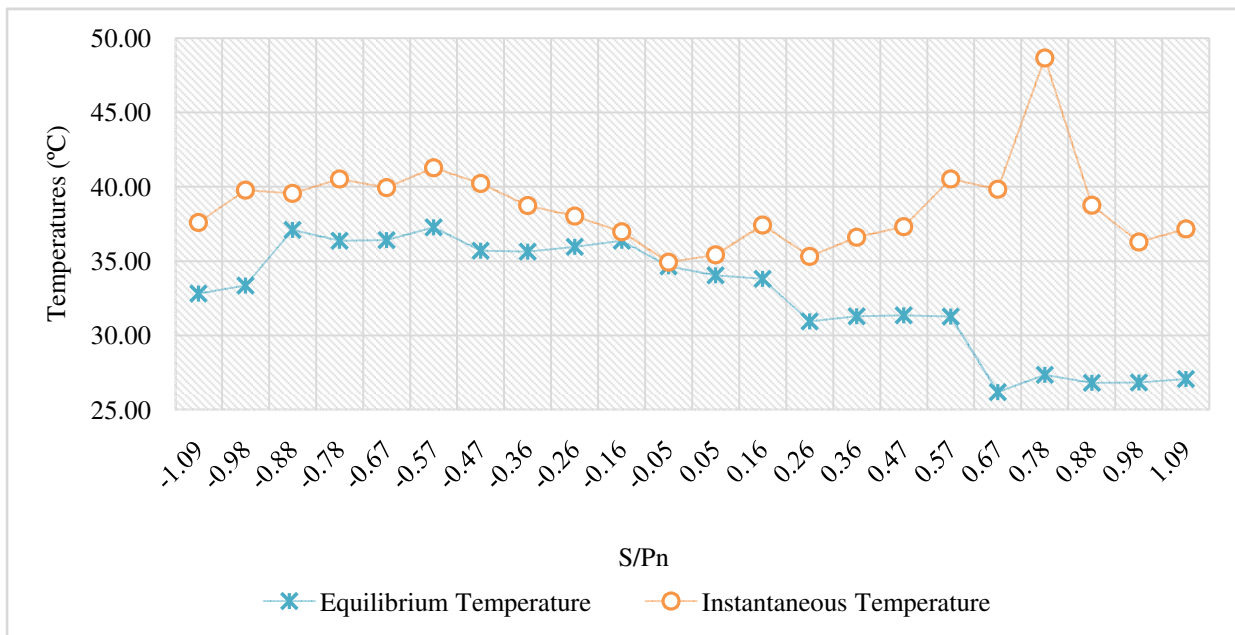


**Figure-9:** Instantaneous and equilibrium temperature variation on the pinion (4% wear).

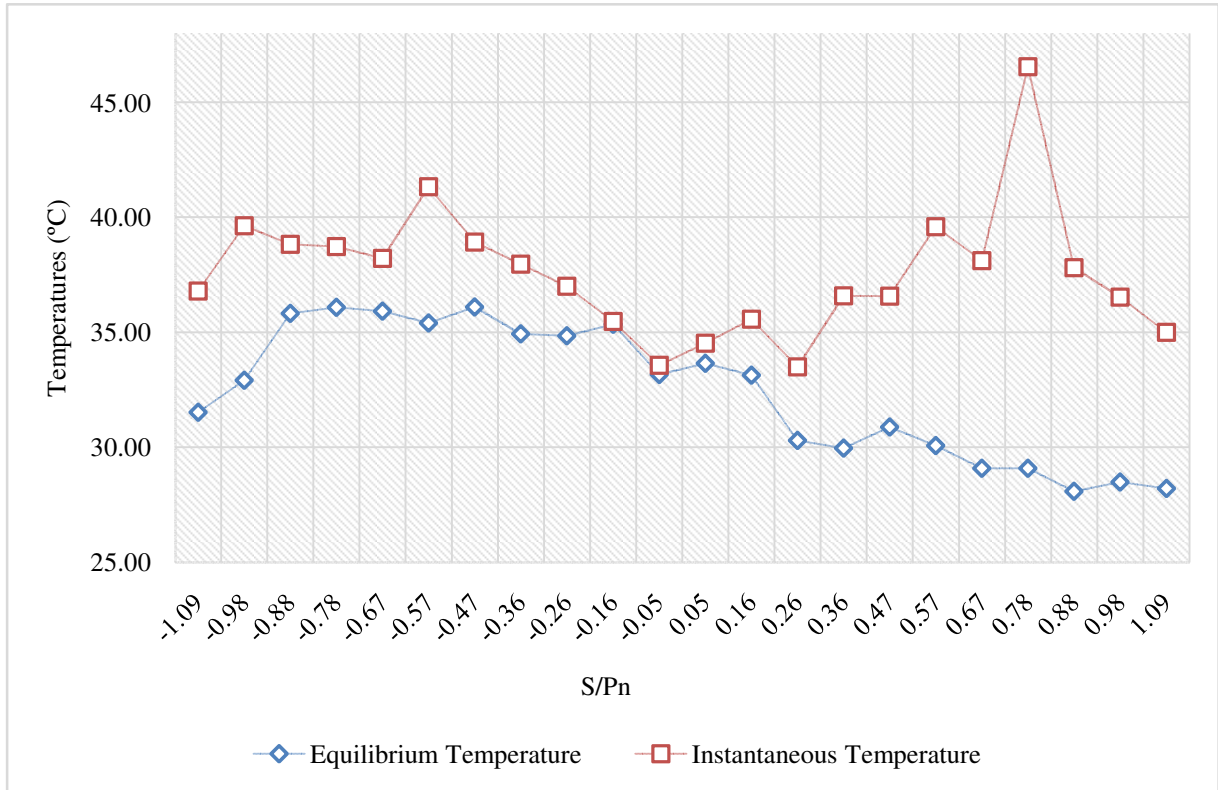


Figure-10: Instantaneous and equilibrium temperature variation on the pinion (8% wear).

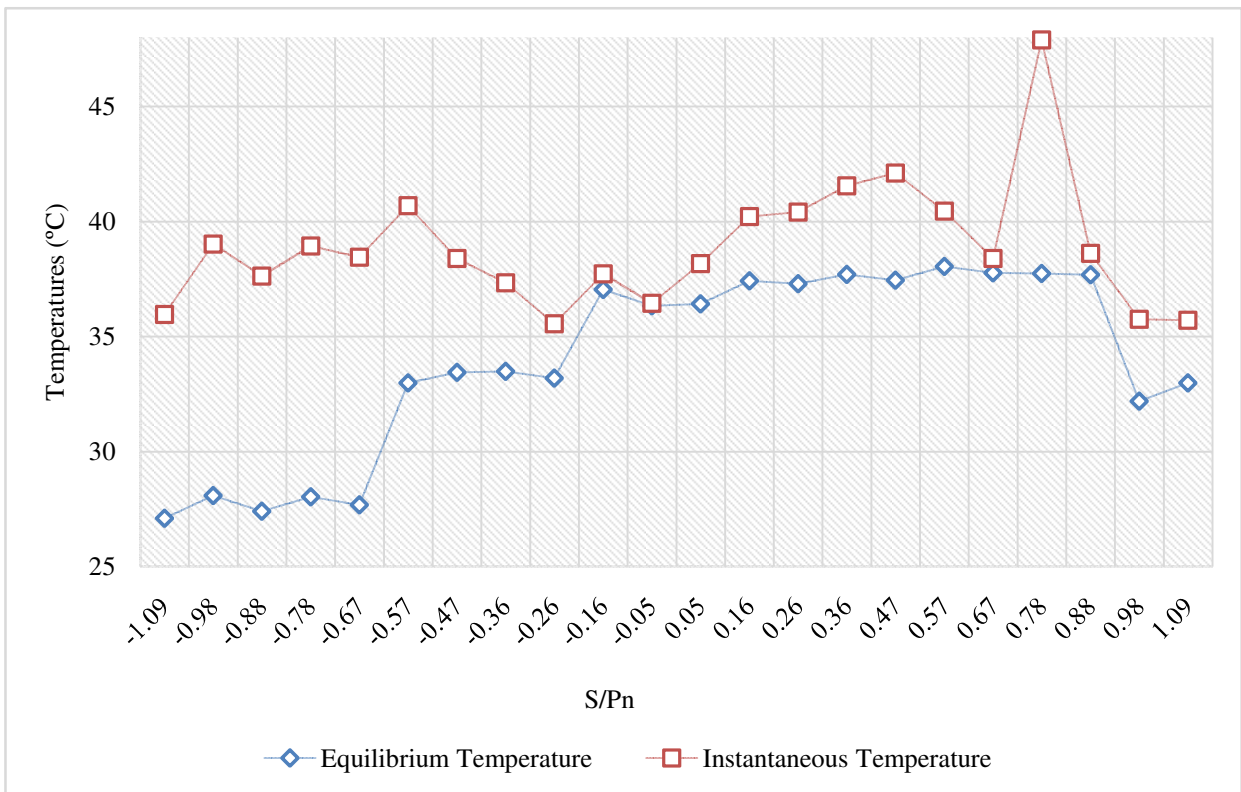


Figure-11: Instantaneous and equilibrium temperature variation on the wheel (0% wear).

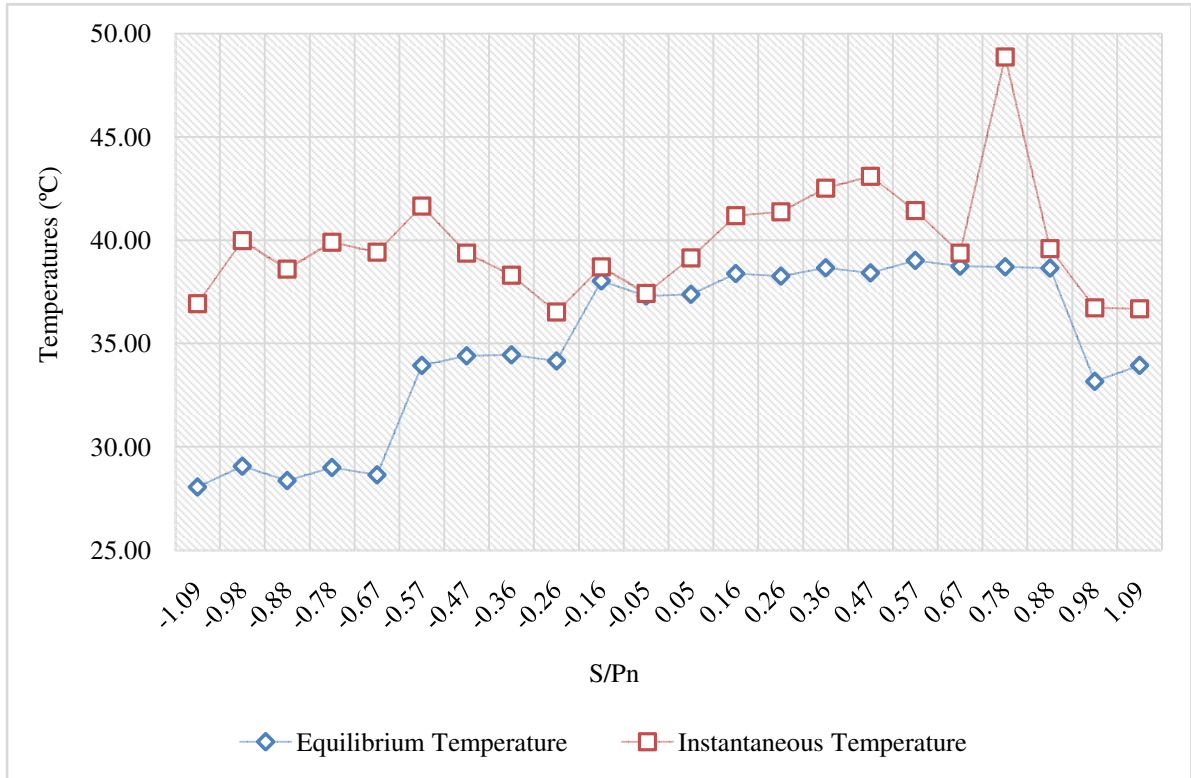


Figure-12:

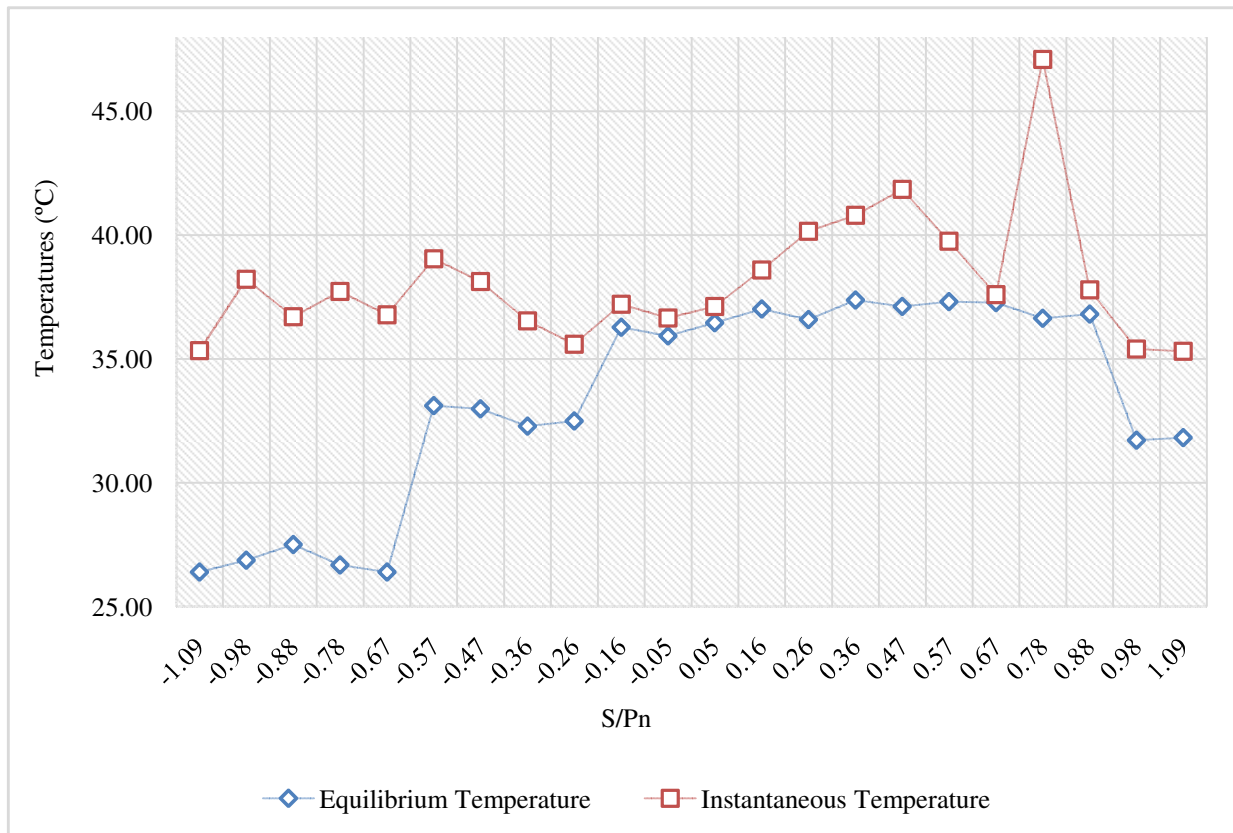


Figure-13: Instantaneous and equilibrium temperature variation on the wheel (8% wear).



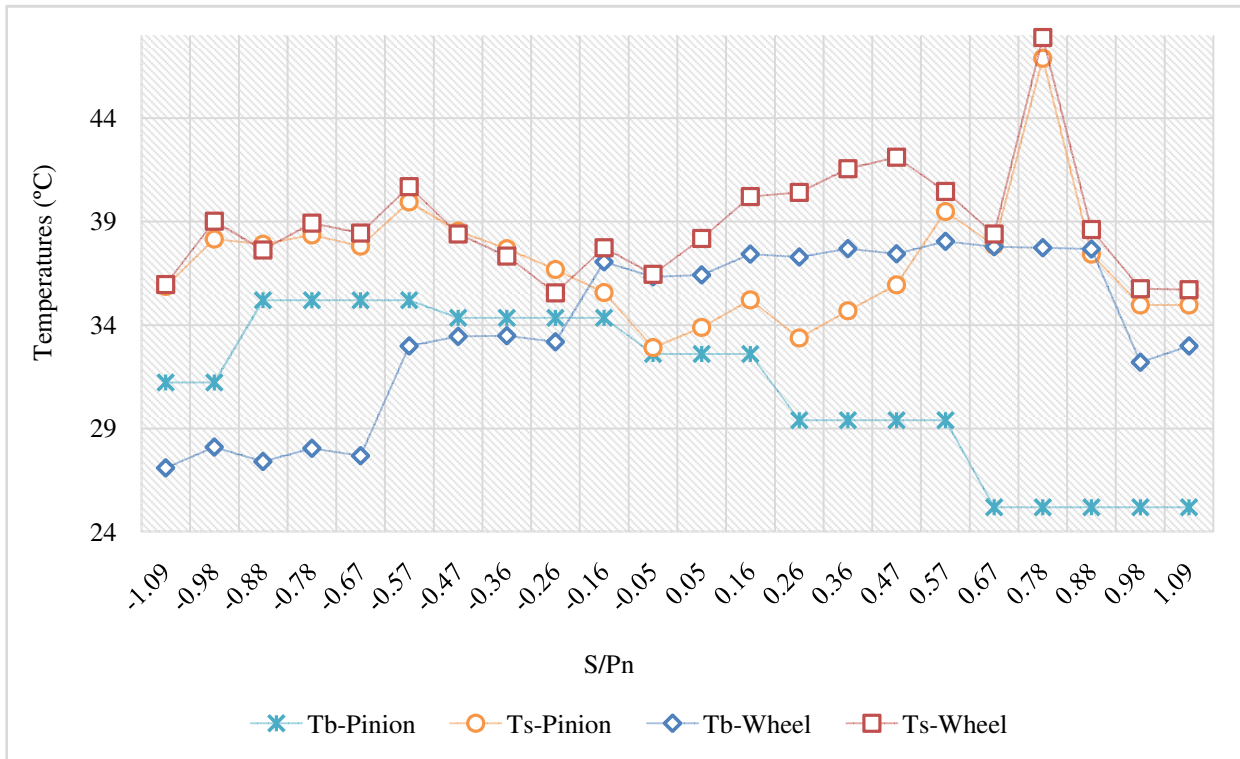


Figure-14: Instantaneous and equilibrium temperature variation on the pinion and the wheel (0% wear).

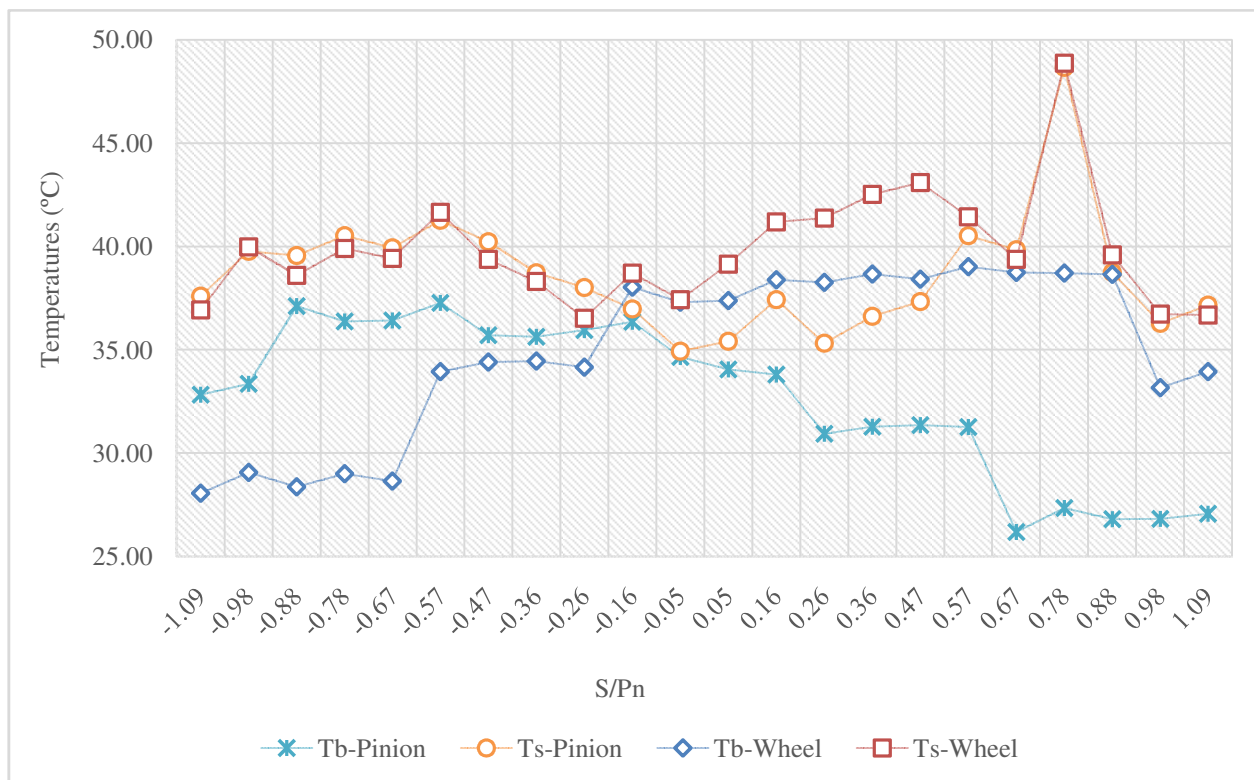


Figure-15: Instantaneous and equilibrium temperature variation on the pinion and the wheel (4% wear).

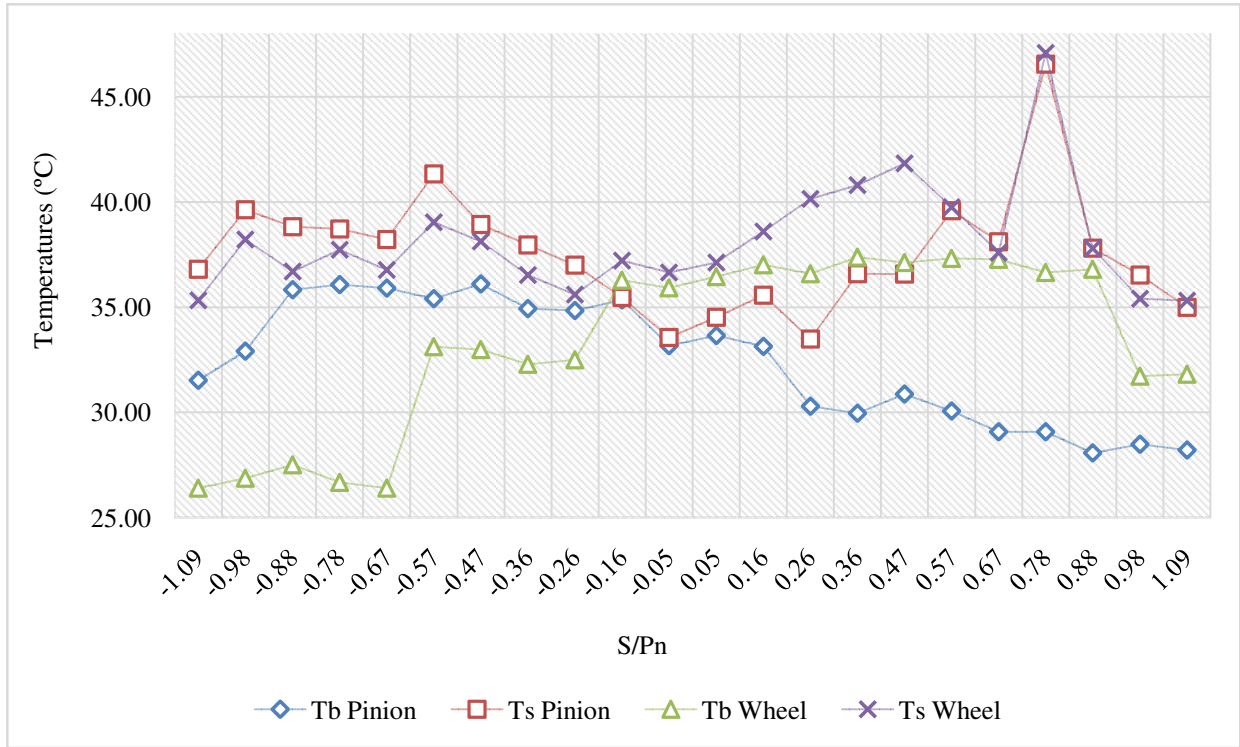


Figure-16: Instantaneous and equilibrium temperature variation on the pinion and the wheel (8% wear).

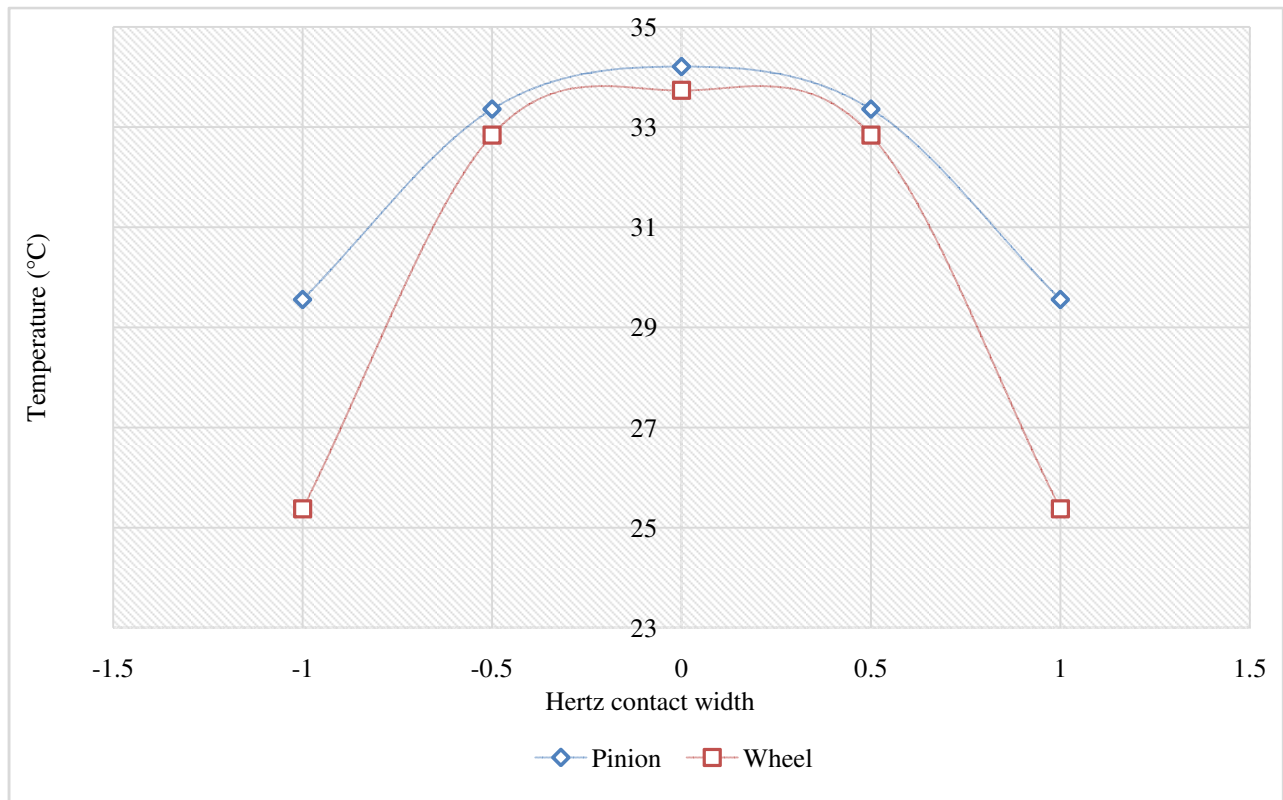
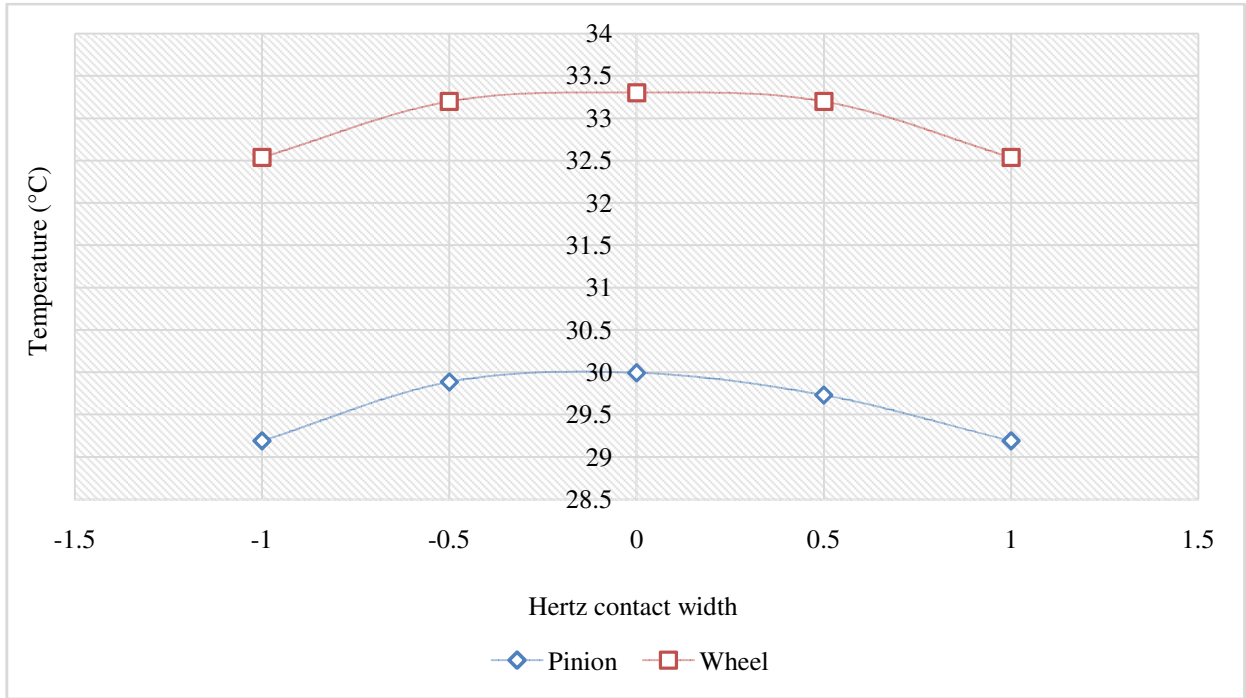
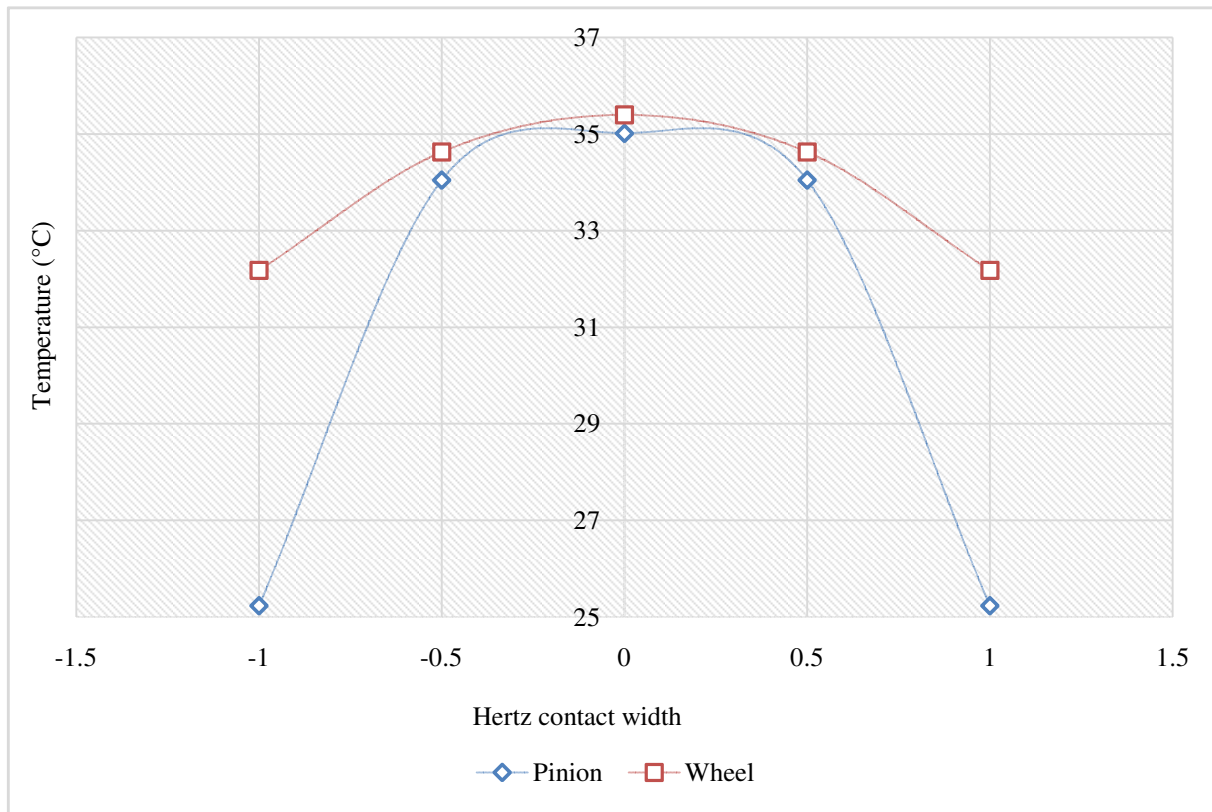


Figure-17: Evolution of surface instantaneous temperature on Hertz contact width at the head.



**Figure-18:** Evolution of surface instantaneous temperature on Herzt contact width at the primitive point.



**Figure-19:** Evolution of surface instantaneous temperature on Herzt contact width at the root.

The results of simulations are presented firstly as a first series of curves for the pinion and the wheel (Figure-8 to Figure-16) where the evolution of the equilibrium temperature as well as that of the instantaneous temperature on the profile of the tooth is shown as a function of  $S/p_n$ , normalized position of the contact point, identified along the line of action.

On the other hand, a second series of curves (Figure-17 to Figure-19) shows the distribution of the local instantaneous temperature  $T_{son}$  the Hertz contact width as a function of the position of the contact point along this width.

For the above conditions, the equilibrium temperature at the head of the wheel tooth is greater than that calculated at the head of the pinion tooth (Figure-14, 15 and 16); this is due to the distribution of the heat transfer coefficient according to the profile of each of the teeth. This reason also explains the superiority of the value of the temperature at the foot of the pinion (Figure-8, 9 and 10) on that of the wheel (Figure-11, 12 and 13).

Indeed, as shown in Table-1, the value of  $h_1$  is higher than that of  $h_4$ ; this influences the value of the temperature at the foot of the teeth. In the same way,  $h_2$  is greater than  $h_3$  and this inequality affects the temperature at the tooth head of the pinion and the wheel as indicated.

The low values of  $h_3$  and  $h_4$ , relative to  $h_2$  and  $h_1$ , respectively, result in a slower fall in temperature from the foot to the head on the tooth of the wheel compared to that observed on the tooth of the pinion.

In general, the instantaneous surface temperature has less variation depending on whether it is calculated on the pinion or the wheel as a function of the value of  $S/P_n$ . However, on approach, the pinion has a higher equilibrium temperature than the wheel. During the withdrawal, the opposite phenomenon is observed, the wheel having a higher temperature than the pinion.

The value of the instantaneous temperature passes through a maximum during the approach, near the theoretical contact start point (point -0.57, Figure-8 to 13); in addition, another maximum is encountered during the withdrawal, near the theoretical end point of contact (point 0.78, Figure-8 to 13) for this temperature. In both cases of maximum, the temperature values on the pinion and on the wheel are practically merged, as shown in Figure-14 to Figure-16.

The peaks observed at +0.78 in Figures 8-16 are due to the increase of the instantaneous sliding speed near the theoretical end point of contact. This increase in speed causes that of frictional heat.

## Conclusion

From the Matlab program written by Mijiyawa on the basis of the simplified model of Koffi which predicts the equilibrium temperature, we have added, still in Matlab, the determination of the instantaneous temperature and all this by including the variation of the wear rate.

The results of these simulations, presented in the form of a series of curves (Figure-8 to 16), show the evolution of the equilibrium temperature, as well as that of the instantaneous temperature on the tooth profile in function of  $S/p_n$  and wear rate.

On the other hand, a second series of curves (Figure-17 to Figure-19) shows the distribution of the local instantaneous temperature  $T_{son}$  the Hertz contact width as a function of the position of the contact point along this width. The general shape of the temperature curves that we have obtained are the same as that made by Koffi on the acetal<sup>7</sup>.

## References

1. Migneault S., Koubaa A., Erchiqui F., Chaala A., Englund K. and Wolcott M.P. (2011). Application of micromechanical models to tensile properties of wood-plastic composites. *Wood Science and Technology*, 45(3), 521-532.
2. Lee S.Y., Yang H.S., Kim H.J., Jeong C.S., Lim B.S. and Lee J.N. (2004). Creep behavior and manufacturing parameters of wood flour filled polypropylene composites. *Composite Structures*, 65(3-4), 459-469.
3. Mendez J.A., Vilaseca F., Pelach M.A., Lopez J.P., Barbera L., Turon X. and Mutje P. (2007). Evaluation of the reinforcing effect of ground wood pulp in the preparation of polypropylene-based composites coupled with maleic anhydride grafted polypropylene. *Journal of Applied Polymer Science*, 105(6), 3588-3596.
4. Aggarwal P.K., Chauhan S., Raghu N., Karmarkar S. and Shashidhar G.M. (2013). Mechanical properties of bio-fibers-reinforced high-density polyethylene composites: effect of coupling agents and bio-fillers. *Journal of Reinforced Plastics and Composites*, 32(22), 1722-1732.
5. Bravo A., Koffi D., Toubal L. and Erchiqui F. (2015). Life and damage mode modeling applied to plastic gears. *Engineering Failure Analysis*, 58, 113-133.
6. Strickle E. and Hachmann H. (1968). Design of Nylon Gears. *Proceedings of the Society of plastics Engineers Annual Technology Conference*, 26, 512-519.
7. KOFFI D. (1987). Study of the thermal behavior of the straight cylindrical plastic gear. *PhD Thesis*. Department of Mechanical Engineering, Polytechnic School of Montreal, Canada.

8. Mao K., Li W., Hooke C.J. and Walton D. (2010). Polymer gear surface thermal wear and its performance prediction. *Tribology International*, 43(1-2), 433-439.
9. Koffi D. and Yelle H. (1991). Simplified model of analysis and computer simulation of the thermal behavior of straight plastic cylindrical gears. II: Results and simulation. *International Journal of CAD / CAM and Computer Graphics*, 6(3-4), 227-261.
10. Sell D.J. (1992). Finite element modeling spur and helical gears in contact. *SAE transactions*, 101(2), 697-703.
11. Akozan M. (1982). Experimental study of the convective heat transfer coefficient for thermoplastic straight cylindrical gears. *Montreal Polytechnic School Montreal*.
12. Mijiyawa F. (2017). Formulation, characterization, modeling and prediction of the thermomechanical behavior of plastic parts and composites of wood fibers: Application to gears. *PhD Thesis*, University of Québec à Trois Rivières, Canada.
13. Tobe T. and Kato M. (1974). A Study on Flash Temperatures. *Trans. ASME, J. Eng. for Ind*, 96, 78-84.